

Natura Non Facit Saltum: An Analytical Model of Smooth Slow-Roll to Ultra-Slow-Roll Transition

Diego Cruces^{1,*}, Minxi He^{2,†}, Shi Pi^{1,3,‡}, Jianing Wang^{3,§}, Masahide Yamaguchi^{4,5,6,¶} and Yuhang Zhu^{4,**}

¹ *Institute of Theoretical Physics, Chinese Academy of Sciences, Beijing 100190, China*

² *Particle Theory and Cosmology Group, Center for Theoretical Physics of the Universe, Institute for Basic Science (IBS), Daejeon, 34126, Korea*

³ *Kavli Institute for the Physics and Mathematics of the Universe (WPI), UTIAS, The University of Tokyo, Kashiwa, Chiba 277-8583, Japan*

⁴ *Cosmology, Gravity, and Astroparticle Physics Group, Center for Theoretical Physics of the Universe, Institute for Basic Science (IBS), Daejeon, 34126, Korea*

⁵ *Department of Physics, Institute of Science Tokyo, 2-12-1 Ookayama, Meguro-ku, Tokyo 152-8551, Japan*

⁶ *Department of Physics and IPAP, Yonsei University, 50 Yonsei-ro, Seodaemun-gu, Seoul 03722, Korea*

(Dated: March 19, 2026)

In this *letter*, we propose a single-field inflation model that realizes a slow-roll-to-ultra-slow-roll transition while keeping the second slow-roll parameter smoothly varying throughout. The model is built through a minimal modification by introducing a simple time dependence in the effective mass term of the Mukhanov-Sasaki equation. We obtain fully analytical solutions for both the background evolution and the curvature perturbations, which makes the parameter dependence of the curvature power spectrum easy to track. To the best of our knowledge, this is the first analytical model that describes a *smooth* transition of this kind. We also compare its signatures with those of the corresponding sharp-transition counterpart.

Introduction— One of the most profound ideas in modern cosmology is that the structure of the Universe we observe today can be traced back to quantum fluctuations in the very early period, most commonly described within the inflationary paradigm [1–3]. The anisotropies of the cosmic microwave background (CMB) and the formation of large-scale structure are among its best known imprints. On much smaller scales, primordial fluctuations may also give rise to primordial black holes (PBHs) [4–7] as well as induced gravitational waves (IGWs) [8–18], both of which have important implications for dark matter, super-massive black holes, GW events observed by LIGO–Virgo–KAGRA, stochastic GW background, energetic cosmic rays, and Hawking radiation [19–37]. A significant amount of PBHs and IGWs can be produced if large curvature perturbations are abundantly generated during inflation [38–67], which can be realized when inflation has experienced an intermediate ultra-slow-roll (USR) phase [68–94].

To obtain reliable predictions from USR inflation without introducing spurious artifacts, the transition between slow-roll (SR) and USR phases must be handled carefully. In most existing studies, however, the second SR parameter ϵ_2 jumps discontinuously at the SR-USR transition [74, 95–100]. Such a discontinuity is physically unnatural and enters directly into the equation of motion for

the curvature perturbation. For instance, a discontinuous transition leads to instantaneous mode mixing in the curvature perturbations, as the Mukhanov-Sasaki (MS) equation is solved separately on the two sides of the transition. The resulting effect is therefore an artifact of the abrupt transition, rather than a genuine consequence of the underlying physical dynamics.

In contrast, the transition can proceed smoothly, as in models with an inflection-point potential [72, 101, 102] or multi-field inflation scenarios [53]. A smooth transition avoids spurious effects, retaining only the physical features. The evolution of both background and perturbations in smooth-transition models has been studied numerically [72, 73, 103–108]. These studies show that a smooth transition can leave distinct imprints on the curvature power spectrum [109–111]. In particular, the amplitude and tilt of the spectrum are determined by the time evolution of the second slow-roll parameter, the inflaton velocity, and the duration of the USR phase [112–114]. Further developments along this direction include numerical computation of bispectrum [42, 115, 116], stochastic inflation approach [82, 117–119], and multi-field embeddings [53, 120].

Despite extensive works on USR inflation, an analytically solvable USR model with a smooth SR-USR transition is still missing. Previous studies address at most one of them: either analytically tractable [60, 83, 85–87, 97, 100, 121, 122] or smoothly evolving [38, 42, 45, 47, 72–77, 101, 105–107, 109, 111, 113, 116, 119, 123–131]. The aim of this paper is to fill this gap by constructing a model that satisfies both requirements. Specifically, we consider the inflationary scenario with a three-stage evolution: an SR phase (SR1) followed by a USR phase,

* dcruces@itp.ac.cn

† heminxi@ibs.re.kr

‡ shi.pi@itp.ac.cn

§ jianing.wang@ipmu.jp

¶ gucci@ibs.re.kr

** yhzhu@ibs.re.kr

which finally ends with another SR phase (SR2). *Nature does not make jumps*, so we require the transitions among these phases to be *smooth*. Simultaneously, we aim for an *analytically* solvable model, in the sense that both the slow-roll parameters and the primordial power spectrum can be expressed in terms of elementary or special mathematical functions. Such a setup will not only simplify practical applications but also make the underlying physics more transparent.

The Model— Here, we specify the criteria of our construction to make the model both *analytic* and *smooth*:

- (i) The second slow-roll parameter ϵ_2 evolves as a continuously differentiable function ($\epsilon_2 \in C^1$), from the first SR stage compatible with CMB constraints (i.e. with $\epsilon_2 \simeq 0$) into a USR regime.
- (ii) ϵ_2 exits the USR regime with a bounded and continuous first derivative and reaches an attractor solution, thereby allowing inflation to end.
- (iii) Both slow-roll parameters and the power spectrum of curvature perturbation admit analytical expressions.

Throughout the three stages, the MS variable v_k always satisfies the following equation [132, 133]

$$v_k'' + \left(k^2 - \frac{\nu^2 - 1/4}{\tau^2} \right) v_k = 0, \quad (1)$$

where the effective index ν is defined through $\nu^2 \equiv 1/4 + (z''/z)\tau^2$, and $z \equiv (a\phi')/\mathcal{H}$ is determined by the evolution of the inflaton background ϕ . All the primes represent derivatives with respect to the conformal time τ . $\mathcal{H} \equiv a'/a$ is the conformal Hubble parameter. In general, ν can be an arbitrary time-dependent function, depending on the inflaton dynamics.

Assuming the first slow-roll parameter $\epsilon_1 \equiv 1 - \mathcal{H}'/\mathcal{H}^2$ is always negligible before the end of inflation (will be verified later), ν can be expressed as [134–136]

$$\nu^2 = \frac{9}{4} + \frac{3}{2}\epsilon_2 + \frac{1}{4}\epsilon_2^2 + \frac{1}{2}\frac{\epsilon_2'}{\mathcal{H}} \equiv \frac{9}{4} + \mathcal{F}(\tau), \quad (2)$$

where the second slow-roll parameter $\epsilon_2 \equiv \epsilon_1'/(\mathcal{H}\epsilon_1)$ and $\mathcal{F}(\tau)$ encodes the time dependence. ϵ_2 characterizes the rate of change of ϵ_1 , which is closely related to the amplitude of the curvature perturbation power spectrum. During SR, $|\epsilon_2| \ll 1$, ϵ_1 is almost constant and therefore the curvature perturbation slope evolving on superhorizon scales. However, ϵ_2 becomes negatively large during the USR phase, causing a rapid decay of ϵ_1 and consequently the growth of the curvature perturbation. Consistency with CMB constraints requires an SR phase at CMB scale, during which ϵ_2 remains small and $\nu \simeq 3/2$.

To achieve our goal (iii), Eq. (1) must admit an analytical solution, while the index ν should be simple enough. The simplest choice of a constant $\nu^2 > 0$, as is commonly

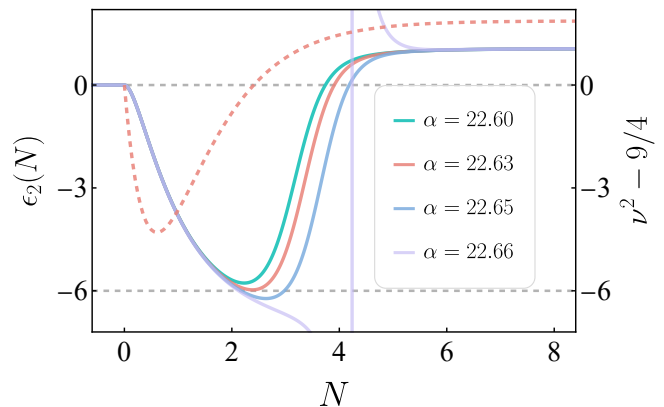


FIG. 1. The evolution of $\epsilon_2(N)$ with different choices of the parameter α , while we fix the combination $(\mu^2 - 9/4)/q^2 = 0.09$. $\nu^2(N) - 9/4$ with $\alpha = 22.63$ and $\mu = 2.0294$ is shown as the red dashed line.

adopted in the literature [71, 87, 91, 93, 118, 131, 137–143], can satisfy (ii) and (i) simultaneously. This is because the solution for $\nu^2 = \text{constant} > 0$ in Eq. (2) is given by hyperbolic functions that have two asymptotic values at $\tau \rightarrow -\infty$ and $\tau \rightarrow 0$ with $\epsilon_2(\tau \rightarrow -\infty) \leq \epsilon_2(\tau \rightarrow 0)$. Given that $\epsilon_2^{\text{USR}} < \epsilon_2^{\text{SR}}$, it is impossible to match it with SR on both sides. If $\nu^2 = \text{constant} < 0$ [91], the solution is given by tangent functions which are not desirable for our purpose.

The next simplest yet sufficiently general option is a polynomial function of time,

$$\mathcal{F}(\tau) = \left(\mu^2 - \frac{9}{4} \right) - \alpha \left(\frac{\tau}{\tau_*} \right) + q^2 \left(\frac{\tau}{\tau_*} \right)^2, \quad (3)$$

which is the model we consider in this *letter*. Here we keep only the first two powers of τ , since higher power terms such as $\propto \tau^3$ modify the behavior of Eq. (1) as they will dominate over k^2 at the far past, while negative powers of τ alter the super-horizon behaviors. There are three independent dimensionless parameters in our model, μ , α , and q , all of which are assumed to be positive. Continuity of ν at the SR1-USR transition time τ_* requires $\mathcal{F}(\tau_*) = 0$, which reduces the number of independent parameters by one via the following constraint on the parameters

$$\mu^2 = \frac{9}{4} + \alpha - q^2. \quad (4)$$

As we will see, the two independent parameters control how inflation ends and the duration of the non-attractor regime with $\epsilon_2 < -3$.

As mentioned above, throughout this paper we will neglect $\mathcal{O}(\epsilon_1)$ corrections (see App. C for details), meaning the Hubble parameter during inflation will be a constant H_0 . With this simplification, Eq. (2) can be rewritten in terms of the e -fold number N as

$$\frac{3}{2}\epsilon_2 + \frac{1}{4}\epsilon_2^2 + \frac{1}{2}\frac{d\epsilon_2}{dN} = \left(\mu^2 - \frac{9}{4} \right) - \alpha e^{-N} + q^2 e^{-2N}, \quad (5)$$

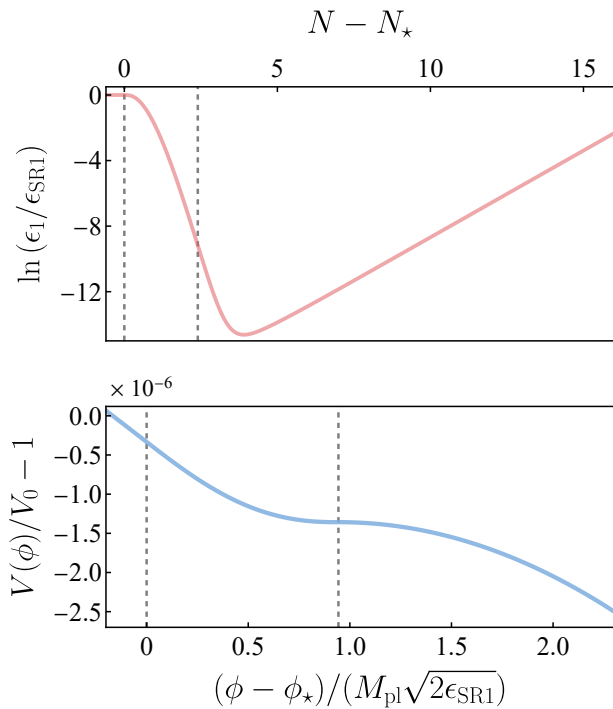


FIG. 2. *Top*: The evolution of the leftmost slow-roll parameter $\epsilon_1(N)$. *Bottom*: The inflaton potential $V(\phi)$ of our model. The first dashed line (the origin of the horizontal axis) marks the time τ_* and the other one indicates when ϵ_2 reaches value -6 . By setting $\epsilon_2 = -6$ and $d\epsilon_2/dN = 0$ in Eq. (5), the e -fold number corresponding to $\epsilon_2 = -6$ is given as $N = -\ln[\alpha/(\alpha - \mu^2 + 9/4) - 1]$. The parameters used in these plots are $\alpha = 22.63$ and $\mu = 2.0294$ and $\epsilon_{\text{SR1}} = 10^{-6}$.

where we have used $a = -1/H_0\tau$ and $N = -\ln(\tau/\tau_*)$. The differential equation Eq. (5) can be solved analytically for ϵ_2 , and the result is presented in App. A. So far, we have achieved the first half of (iii).

We plot ϵ_2 in Fig. 1 for several representative parameter choices. Clearly, ϵ_2 evolves smoothly from its SR1 value ($\epsilon_2^{\text{SR1}} \simeq 0$) to its final SR2 value ($\epsilon_{2,f} \simeq -3 + 2\mu$), with an intermediate USR (or non-attractor) phase where $-3 > \epsilon_2 > -3 - 2\mu$, satisfying in this way our conditions (i) and (ii). In Fig. 1 we can also see that if we choose parameters such that $\epsilon_2 < -3 - 2\mu$ at some point in its evolution (purple line), it becomes discontinuous and hence not desirable for our purposes. For reference, we also plot the corresponding function $\nu^2(N)$.

Power Spectrum and Features— To fully achieve (iii), we need to solve the mode function $v_k(\tau)$ and function $z(\tau)$ analytically to obtain the curvature perturbation $\mathcal{R}_k = v_k/z$.

By inserting Eq. (3) into Eq. (1), $v_k(\tau)$ admits a general solution in terms of the Whittaker- M and W functions:

$$v_k(\tau) = \mathcal{C}_1 \cdot W_{i\tilde{\alpha},\mu}(2ik_{\text{eff}}\tau) + \mathcal{C}_2 \cdot M_{i\tilde{\alpha},\mu}(2ik_{\text{eff}}\tau), \quad (6)$$

where we introduced $k_* \equiv -1/\tau_*$, $k_{\text{eff}}^2 \equiv k^2 - (qk_*)^2$, and $\tilde{\alpha} \equiv \alpha k_*/2k_{\text{eff}}$. The coefficients $\mathcal{C}_{1,2}$ will be determined later by appropriate boundary conditions.

According to Eqs. (2) and (3), function $z(\tau)$ satisfies

$$\frac{1}{4} + \frac{z''}{z}\tau^2 = \mu^2 - \alpha \left(\frac{\tau}{\tau_*}\right) + q^2 \left(\frac{\tau}{\tau_*}\right)^2. \quad (7)$$

This equation can also be solved analytically and expressed by the same types of special functions as

$$z(\tau) = \mathcal{B}_1 \cdot W_{\alpha/2q,\mu}(2q\tau/\tau_*) + \mathcal{B}_2 \cdot M_{\alpha/2q,\mu}(2q\tau/\tau_*). \quad (8)$$

Given the relation $z(\tau) \approx -\sqrt{2\epsilon_1(\tau)}M_{\text{pl}}/(H_0\tau)$, the coefficients $\mathcal{B}_{1,2}$ can be determined by boundary conditions $\epsilon_1|_{\tau_*} = \epsilon_{\text{SR1}}$, $\epsilon_1'|_{\tau_*} = 0$, which are imposed by smooth connection between SR1 and USR. Here ϵ_{SR1} denotes the first slow-roll parameter during SR1 that is related to the amplitude of CMB-measured power spectrum of curvature perturbation via $\mathcal{P}_{\mathcal{R}}^{\text{SR1}} = H^2/(8\pi^2\epsilon_{\text{SR1}}M_{\text{pl}}^2)$. The explicit expressions for the coefficients are collected in App. A. The analytical result of $\epsilon_1(N)$ follows right after fixing the exact form of $z(\tau)$ in Eq. (8). The corresponding potential can be reconstructed using $V = M_{\text{pl}}^2 H^2 (3 - \epsilon_1)$, with $H = H_0 \exp(-\int \epsilon_1 dN)$. The results of ϵ_1 and $V(\phi)$ are presented in Fig. 2.

Combining Eqs. (6) and (8), we arrive at the following analytical expression for the curvature perturbation,

$$\mathcal{R}_k = \frac{\mathcal{C}_1 W_{i\tilde{\alpha},\mu}(2ik_{\text{eff}}\tau) + \mathcal{C}_2 M_{i\tilde{\alpha},\mu}(2ik_{\text{eff}}\tau)}{\mathcal{B}_1 W_{\alpha/2q,\mu}(2q\tau/\tau_*) + \mathcal{B}_2 M_{\alpha/2q,\mu}(2q\tau/\tau_*)}. \quad (9)$$

During SR1, it should recover the Bunch-Davies (BD) solution

$$\mathcal{R}_k^{\text{BD}} = \frac{H}{M_{\text{pl}}\sqrt{\epsilon_{\text{SR1}}}} \frac{i}{2\sqrt{k^3}} (1 + ik\tau)e^{-ik\tau}, \quad (10)$$

so our boundary conditions are

$$\mathcal{R}_k|_{\tau_*} = \mathcal{R}_k^{\text{BD}}|_{\tau_*}, \quad \mathcal{R}'_k|_{\tau_*} = \mathcal{R}_k^{\text{BD}'}|_{\tau_*}, \quad (11)$$

which pin down the coefficients $\mathcal{C}_{1,2}$. The detailed expressions are again collected in App. A. In the limit $\tau \rightarrow 0^-$, the Whittaker- M decays more rapidly than the Whittaker- W . As a result, when evaluating the power spectrum at the end of inflation i.e. $\mathcal{P}_{\mathcal{R}}(k) \equiv (k^3/2\pi^2)|\mathcal{R}_k(0^-)|^2$, it is sufficient to take Eq. (9) as

$$\begin{aligned} \mathcal{R}_k(0^-) &= \lim_{\tau \rightarrow 0^-} \frac{\mathcal{C}_1 \cdot W_{i\tilde{\alpha},\mu}(2ik_{\text{eff}}\tau)}{\mathcal{B}_1 \cdot W_{\alpha/2q,\mu}(2q\tau/\tau_*)} \\ &= \frac{\mathcal{C}_1}{\mathcal{B}_1} \frac{\Gamma(1/2 + \mu - \alpha/2q)}{\Gamma(1/2 + \mu - i\tilde{\alpha})} \left(\frac{-ik_{\text{eff}}}{qk_*}\right)^{\frac{1}{2} - \mu}. \end{aligned} \quad (12)$$

The analytical results are verified in Fig. 3 by comparing them with the numerical results, demonstrating excellent agreement.

These analytical expressions also allow the properties of the final power spectrum in different regions to be readily understood by taking the appropriate limits.

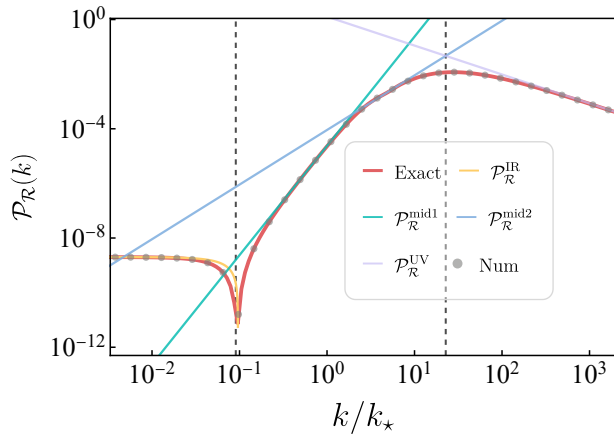


FIG. 3. Comparison of the analytically derived power spectrum (red line) with the approximation formulae in different regions (yellow for the IR region, green and blue for the growth region, purple for the UV region), as well as with the numerical results (gray dots). The dip and the peak location are shown by the black dashed lines. The parameters are set to $\tau_* = -1$, $\alpha = 22.63$ and $\mu = 2.0294$.

- *Infrared (IR) region.* When $k \ll k_*$, we perform a power series expansion around $k/k_* \rightarrow 0$ as

$$\mathcal{P}_{\mathcal{R}}^{\text{IR}}(k) = \frac{a_0 + a_2 k^2}{2\pi^2 |\mathcal{B}_1|^2}, \quad (13)$$

where a_0 and a_2 are specified in Appendix B, where one can check that they are of opposite sign. Due to the sign difference, a dip appears in the power spectrum. Its location can be determined straightforwardly by solving for the zero of the above approximation as

$$k_{\text{dip}} = \left(-\frac{a_0}{a_2} \right)^{1/2}. \quad (14)$$

- *Growth region.* When $k \sim k_*$, our model enters the region exhibiting the k^4 -enhancement [92, 109, 112, 127, 128, 131, 144, 145]. Using the dip location, the power spectrum around this region can be approximated as

$$\mathcal{P}_{\mathcal{R}}^{\text{mid1}}(k) = \mathcal{P}_{\mathcal{R}}^{\text{SR1}} \left(\frac{k}{k_{\text{dip}}} \right)^4. \quad (15)$$

However, around $k \sim qk_* > k_*$, we find that the infrared scaling law deviates from k^4 and instead approaches to k^2 . We approximate the power spectrum in this region as

$$\mathcal{P}_{\mathcal{R}}^{\text{mid2}}(k) = \mathcal{P}_{\mathcal{R}}(qk_*) \left(\frac{k}{qk_*} \right)^2, \quad (16)$$

where the closed form for $\mathcal{P}_{\mathcal{R}}$ at $k = qk_*$ can be found in Eq. (B7).

- *Ultraviolet (UV) region.* For modes exiting the horizon at very late stages, in the limit $k \gg k_*$, we have $|\mathcal{C}_1(k)| \sim 1/\sqrt{2k}$ and $k_{\text{eff}} \sim k$. The dimensionless power spectrum is approximated by

$$\mathcal{P}_{\mathcal{R}}^{\text{UV}}(k) = \frac{k^2}{4\pi^2} \left(\frac{k}{qk_*} \right)^{1-2\mu} \frac{\Gamma(1/2 + \mu - \alpha/2q)^2}{|\mathcal{B}_1|^2 \Gamma(1/2 + \mu)^2}. \quad (17)$$

Therefore, the UV scaling behaves as $k^{3-2\mu}$, and it becomes scale-invariant when $\mu = 3/2$, as expected.

Making use of these formulae, we can estimate the peak location by solving for the intersection point of Eq. (16) and Eq. (17), which gives

$$k_{\text{peak}} = \left[\frac{(qk_*)^{2\mu+1}}{4\pi^2 \mathcal{P}_{\mathcal{R}}(qk_*)} \frac{\Gamma(\frac{1}{2} + \mu - \alpha/2q)^2}{|\mathcal{B}_1|^2 \Gamma(\frac{1}{2} + \mu)^2} \right]^{\frac{1}{2\mu-1}}. \quad (18)$$

In Fig. 3, we compare the approximation formulae in different regions with the exact result from Eq. (12). The estimated locations of the dip and the peak, indicated by the black dashed lines, are obtained from Eq. (14) and Eq. (18), respectively. They are all in excellent agreement with the exact curve.

Comparison with Transient Model— A natural next step is to examine how it contrasts with models characterized by sharp transitions. In this section, we compare our model with its sharp counterpart which we refer to as the transient model. In this model, ϵ_2 is defined by the following piecewise function,

$$\epsilon_2(N) = \begin{cases} 0 & N < N_1, \\ -6 & N_1 < N < N_1 + N_{\text{eff}}, \\ \epsilon_{2,f} & N > N_1 + N_{\text{eff}}, \end{cases} \quad (19)$$

here $\epsilon_{2,f} \equiv 2\mu - 3$ is the asymptotic value of our solution ϵ_2 in Eq. (A1) at the end of SR2 phase. We use N_1 to denote the time when the smooth model enters the non-attractor phase $\epsilon_2 < -3$, while N_{eff} is the effective duration of the USR phase, defined as

$$N_{\text{eff}} \equiv -\frac{1}{6} \int_{\epsilon_2 < -3} \epsilon_2(N) dN + \frac{1}{3} \ln \frac{4\mu}{2\mu + 3}. \quad (20)$$

For later convenience, we introduce the shorthand notations \bar{N}_{eff} and ΔN to denote the first and second terms in Eq. (20) respectively. \bar{N}_{eff} has a transparent interpretation: $6 \times \bar{N}_{\text{eff}}$ is exactly the area of the green-shaded region in Fig. 4, namely where the smooth model remains in the $\epsilon_2 < -3$ regime. The detailed meaning and implications were investigated in Ref. [121] for the models ending with $\epsilon_{2,f} = 0$, where the peak amplitude is estimated as $(e^{6\bar{N}_{\text{eff}}} \times 2.61 \times 4) \mathcal{P}_{\mathcal{R}}^{\text{SR1}}$. In transient models, $\epsilon_{2,f}$ affects both the location of the dip and the height of the peak. To incorporate these effects, we introduce ΔN , which vanishes for $\epsilon_{2,f} = 0$ (equivalently, $\mu = 3/2$). With this additional term, a general transient model with

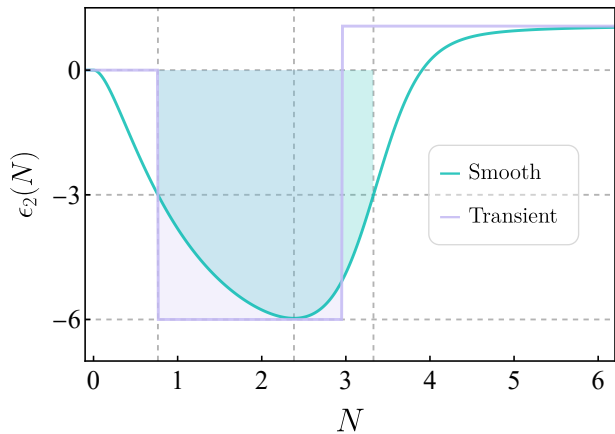


FIG. 4. The comparison of $\epsilon_2(N)$ between our smooth model (green line) and the transient model (purple line). For the smooth one we take $\alpha = 22.63$ and $\mu = 2.0294$, while the transient one is specified by Eq. (19). The shaded regions correspond to the areas where the models enter the non-attractor phase.

non-zero $\epsilon_{2,f}$ can be mapped onto the special case with $\epsilon_{2,f} = 0$ such that both the dip position and the peak amplitude are matched exactly.

In Fig. 5, we compare the power spectrum from our smooth model with that of the transient model, whose ϵ_2 is given by Eq. (19). These two models agree perfectly in the IR limit, including the dip position. The peak amplitude differs slightly, by roughly a factor of ~ 1.4 . However, the peak position is noticeably shifted due to the different growth behavior discussed in the previous section. More importantly, the disagreement becomes significant in the UV tail, where the amplitudes differ by factors of $\mathcal{O}(10)$ to $\mathcal{O}(10^2)$. The enhanced UV end of the power spectrum or oscillatory UV features can be easily tested through the associated IGW signals. We leave the detailed investigation of these observational consequences to future work. Finally, for future reference, we also list in Table I several representative cases, beyond the parameter choices considered in the main text, for which the minimum value of ϵ_2 is -6 . These cases are subject to observational constraints on the PBH abundance.

Summary— In this work, we show, to the best of our knowledge, the first analytically solvable single-field inflation model that allows a smooth SR-USR-SR transition without introducing any discontinuity in the second slow-roll parameter ϵ_2 . This is realized by a simple ansatz that the effective mass term in the MS equation is a polynomial in time. In contrast to previous numerical studies [42, 75, 106, 107, 129, 130, 146, 147], the analytical tractability of our model makes it straightforward to trace both the parameter dependence and the behavior of the power spectrum across different regimes. We further uncover a simple correspondence between our smooth-transition model and the conventional sharp-transition

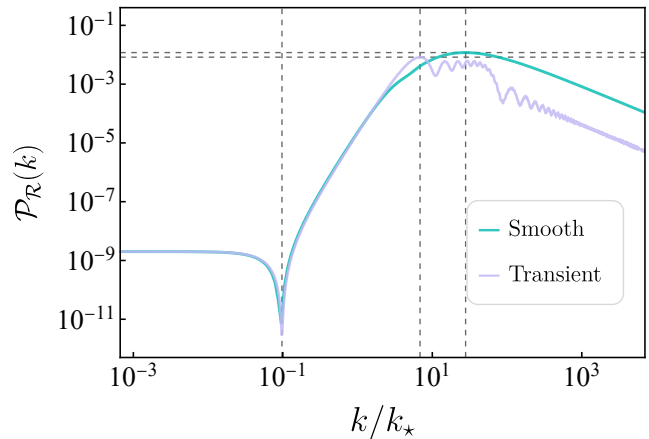


FIG. 5. The comparison of power spectra between our smooth model (green line) with $\tau_* = -1$, $\alpha = 22.63$ and $\mu = 2.0294$, and the transient model (purple line) given by Eq. (19). Horizontal dashed lines denotes the dip and peak positions, while vertical dashed lines show the amplitude of peaks.

USR scenarios. The two share similar features around the dip and yield comparable peak amplitudes, but they differ significantly in the peak location and in the behavior of the UV tail.

This *letter* focused primarily on the analytical solutions of the model. Many aspects remain to be explored in future works, from both phenomenological and theoretical perspectives. For example, it will be interesting to carry out a detailed analysis of the PBHs abundance and the IGWs signals predicted by our setup. As an analytical expression for the power spectrum is available, we expect to have an analytical expression for IGW spectrum, as is done for monochromatic [148, 149], lognormal [43, 150], and broken power-law [151] spectra. Other directions worth investigating include non-Gaussianities, as well as stochastic and quantum effects associated with the model. All of these issues are closely connected to forthcoming observational probes including micro-lensing surveys [152–156], CMB experiments [157–162], and next-generation gravitational-wave detectors [163–170]. Analytical control over full dynamics makes our smooth scenario both a useful theoretical laboratory and a practical framework for connecting small-scale inflationary physics with observations.

Acknowledgements This work is supported by the National Key Research and Development Program of China Grant No. 2021YFC2203004. D.C. is supported by the 78th Batch of General Grants of the China Postdoctoral Science Foundation No. 2025M783447. M.H. is supported by IBS under the project code, IBS-R018-D1. S.P. is supported in part by the National Natural Science Foundation of China (NSFC) Grants No. 12475066, No. 12447101 and JSPS KAKENHI No. 24K00624. J.W. is supported in part by JSPS KAKENHI No. 24K00624 and by Kavli IPMU, which was established by the World Premier International Research Center Initiative (WPI),

MEXT, Japan. M.Y. is supported by IBS under the project code, IBS-R018-D3, and by JSPS Grant-in-Aid

for Scientific Research Number JP23K20843. Y.Z. is supported by IBS under the project code, IBS-R018-D3.

-
- [1] A. A. Starobinsky, “A New Type of Isotropic Cosmological Models Without Singularity,” *Phys. Lett. B* **91** (1980) 99–102.
- [2] K. Sato, “First Order Phase Transition of a Vacuum and Expansion of the Universe,” *Mon. Not. Roy. Astron. Soc.* **195** (1981) 467–479.
- [3] A. H. Guth, “The Inflationary Universe: A Possible Solution to the Horizon and Flatness Problems,” *Phys. Rev. D* **23** (1981) 347–356.
- [4] Y. B. Zel’dovich and I. D. Novikov, “The Hypothesis of Cores Retarded during Expansion and the Hot Cosmological Model,” *Sov. Astron.* **10** (1967) 602.
- [5] S. Hawking, “Gravitationally collapsed objects of very low mass,” *Mon. Not. Roy. Astron. Soc.* **152** (1971) 75.
- [6] B. J. Carr and S. W. Hawking, “Black holes in the early Universe,” *Mon. Not. Roy. Astron. Soc.* **168** (1974) 399–415.
- [7] B. J. Carr, “The Primordial black hole mass spectrum,” *Astrophys. J.* **201** (1975) 1–19.
- [8] K. Tomita, “Non-Linear Theory of Gravitational Instability in the Expanding Universe,” *Prog. Theor. Phys.* **37** no. 5, (1967) 831–846.
- [9] S. Matarrese, O. Pantano, and D. Saez, “A General relativistic approach to the nonlinear evolution of collisionless matter,” *Phys. Rev. D* **47** (1993) 1311–1323.
- [10] S. Matarrese, O. Pantano, and D. Saez, “General relativistic dynamics of irrotational dust: Cosmological implications,” *Phys. Rev. Lett.* **72** (1994) 320–323, [arXiv:astro-ph/9310036](#).
- [11] S. Matarrese, S. Mollerach, and M. Bruni, “Second order perturbations of the Einstein-de Sitter universe,” *Phys. Rev. D* **58** (1998) 043504, [arXiv:astro-ph/9707278](#).
- [12] H. Noh and J.-c. Hwang, “Second-order perturbations of the Friedmann world model,” *Phys. Rev. D* **69** (2004) 104011.
- [13] C. Carbone and S. Matarrese, “A Unified treatment of cosmological perturbations from super-horizon to small scales,” *Phys. Rev. D* **71** (2005) 043508, [arXiv:astro-ph/0407611](#).
- [14] K. Nakamura, “Second-order gauge invariant cosmological perturbation theory: Einstein equations in terms of gauge invariant variables,” *Prog. Theor. Phys.* **117** (2007) 17–74, [arXiv:gr-qc/0605108](#).
- [15] K. N. Ananda, C. Clarkson, and D. Wands, “The Cosmological gravitational wave background from primordial density perturbations,” *Phys. Rev. D* **75** (2007) 123518, [arXiv:gr-qc/0612013](#).
- [16] B. Osano, C. Pitrou, P. Dunsby, J.-P. Uzan, and C. Clarkson, “Gravitational waves generated by second order effects during inflation,” *JCAP* **04** (2007) 003, [arXiv:gr-qc/0612108](#).
- [17] D. Baumann, P. J. Steinhardt, K. Takahashi, and K. Ichiki, “Gravitational Wave Spectrum Induced by Primordial Scalar Perturbations,” *Phys. Rev. D* **76** (2007) 084019, [arXiv:hep-th/0703290](#).
- [18] R. Saito and J. Yokoyama, “Gravitational wave background as a probe of the primordial black hole abundance,” *Phys. Rev. Lett.* **102** (2009) 161101, [arXiv:0812.4339 \[astro-ph\]](#). [Erratum: *Phys.Rev.Lett.* 107, 069901 (2011)].
- [19] A. Barrau, G. Boudoul, F. Donato, D. Maurin, P. Salati, and R. Taillet, “Anti-protons from primordial black holes,” *Astron. Astrophys.* **388** (2002) 676, [arXiv:astro-ph/0112486](#).
- [20] R. Bean and J. Magueijo, “Could supermassive black holes be quintessential primordial black holes?,” *Phys. Rev. D* **66** (2002) 063505, [arXiv:astro-ph/0204486](#).
- [21] N. Duechting, “Supermassive black holes from primordial black hole seeds,” *Phys. Rev. D* **70** (2004) 064015, [arXiv:astro-ph/0406260](#).
- [22] A. T. Kearsley *et al.*, “Analytical scanning and transmission electron microscopy of laboratory impacts on Stardust aluminum foils: Interpreting impact crater morphology and the composition of impact residues,” *Meteorit. Planet. Sci.* **42** (2007) 191, [arXiv:astro-ph/0612013](#).
- [23] B. J. Carr, K. Kohri, Y. Sendouda, and J. Yokoyama, “New cosmological constraints on primordial black holes,” *Phys. Rev. D* **81** (2010) 104019, [arXiv:0912.5297 \[astro-ph.CO\]](#).
- [24] M. Kawasaki, A. Kusenko, and T. T. Yanagida, “Primordial seeds of supermassive black holes,” *Phys. Lett. B* **711** (2012) 1–5, [arXiv:1202.3848 \[astro-ph.CO\]](#).
- [25] M. Sasaki, T. Suyama, T. Tanaka, and S. Yokoyama, “Primordial Black Hole Scenario for the Gravitational-Wave Event GW150914,” *Phys. Rev. Lett.* **117** no. 6, (2016) 061101, [arXiv:1603.08338 \[astro-ph.CO\]](#). [Erratum: *Phys.Rev.Lett.* 121, 059901 (2018)].
- [26] S. Bird, I. Cholis, J. B. Muñoz, Y. Ali-Haïmoud, M. Kamionkowski, E. D. Kovetz, A. Raccanelli, and A. G. Riess, “Did LIGO detect dark matter?,” *Phys. Rev. Lett.* **116** no. 20, (2016) 201301, [arXiv:1603.00464 \[astro-ph.CO\]](#).
- [27] Y. Ali-Haïmoud, E. D. Kovetz, and M. Kamionkowski, “Merger rate of primordial black-hole binaries,” *Phys. Rev. D* **96** no. 12, (2017) 123523, [arXiv:1709.06576 \[astro-ph.CO\]](#).
- [28] J. R. Espinosa, D. Racco, and A. Riotto, “Primordial Black Holes from Higgs Vacuum Instability: Avoiding Fine-tuning through an Ultraviolet Safe Mechanism,” *Eur. Phys. J. C* **78** no. 10, (2018) 806, [arXiv:1804.07731 \[hep-ph\]](#).
- [29] N. Bartolo, V. De Luca, G. Franciolini, M. Peloso, D. Racco, and A. Riotto, “Testing primordial black holes as dark matter with LISA,” *Phys. Rev. D* **99** no. 10, (2019) 103521, [arXiv:1810.12224 \[astro-ph.CO\]](#).
- [30] B. Carr and J. Silk, “Primordial Black Holes as Generators of Cosmic Structures,” *Mon. Not. Roy. Astron. Soc.* **478** no. 3, (2018) 3756–3775,

- [arXiv:1801.00672 \[astro-ph.CO\]](#).
- [31] C. Caprini and D. G. Figueroa, “Cosmological Backgrounds of Gravitational Waves,” *Class. Quant. Grav.* **35** no. 16, (2018) 163001, [arXiv:1801.04268 \[astro-ph.CO\]](#).
- [32] B. Carr, K. Kohri, Y. Sendouda, and J. Yokoyama, “Constraints on primordial black holes,” *Rept. Prog. Phys.* **84** no. 11, (2021) 116902, [arXiv:2002.12778 \[astro-ph.CO\]](#).
- [33] M. Sasaki and J. Wang, “Unveiling primordial black hole relics through induced gravitational waves,” 2025. <https://arxiv.org/abs/2512.22450>.
- [34] P. Petrov and J. Wang, “Bounds on gravitational wave production from unitarity in an early nec-violating model,” 2026. <https://arxiv.org/abs/2601.14008>.
- [35] S. Das and A. Hook, “Black hole production of monopoles in the early universe,” *JHEP* **12** (2021) 145, [arXiv:2109.00039 \[hep-ph\]](#).
- [36] M. He, K. Kohri, K. Mukaida, and M. Yamada, “Formation of hot spots around small primordial black holes,” *JCAP* **01** (2023) 027, [arXiv:2210.06238 \[hep-ph\]](#).
- [37] M. He, K. Kohri, K. Mukaida, and M. Yamada, “Thermalization and hotspot formation around small primordial black holes,” *JCAP* **10** (2024) 080, [arXiv:2407.15926 \[hep-ph\]](#).
- [38] H. Di and Y. Gong, “Primordial black holes and second order gravitational waves from ultra-slow-roll inflation,” *JCAP* **07** (2018) 007, [arXiv:1707.09578 \[astro-ph.CO\]](#).
- [39] R.-g. Cai, S. Pi, and M. Sasaki, “Gravitational Waves Induced by non-Gaussian Scalar Perturbations,” *Phys. Rev. Lett.* **122** no. 20, (2019) 201101, [arXiv:1810.11000 \[astro-ph.CO\]](#).
- [40] N. Bartolo, V. De Luca, G. Franciolini, A. Lewis, M. Peloso, and A. Riotto, “Primordial Black Hole Dark Matter: LISA Serendipity,” *Phys. Rev. Lett.* **122** no. 21, (2019) 211301, [arXiv:1810.12218 \[astro-ph.CO\]](#).
- [41] C. Unal, “Imprints of Primordial Non-Gaussianity on Gravitational Wave Spectrum,” *Phys. Rev. D* **99** no. 4, (2019) 041301, [arXiv:1811.09151 \[astro-ph.CO\]](#).
- [42] H. V. Ragavendra, P. Saha, L. Sriramkumar, and J. Silk, “Primordial black holes and secondary gravitational waves from ultraslow roll and punctuated inflation,” *Phys. Rev. D* **103** no. 8, (2021) 083510, [arXiv:2008.12202 \[astro-ph.CO\]](#).
- [43] S. Pi and M. Sasaki, “Gravitational Waves Induced by Scalar Perturbations with a Lognormal Peak,” *JCAP* **09** (2020) 037, [arXiv:2005.12306 \[gr-qc\]](#).
- [44] G. Domènech, S. Pi, and M. Sasaki, “Induced gravitational waves as a probe of thermal history of the universe,” *JCAP* **08** (2020) 017, [arXiv:2005.12314 \[gr-qc\]](#).
- [45] Q. Wang, Y.-C. Liu, B.-Y. Su, and N. Li, “Primordial black holes from the perturbations in the inflaton potential in peak theory,” *Phys. Rev. D* **104** no. 8, (2021) 083546, [arXiv:2111.10028 \[astro-ph.CO\]](#).
- [46] S. Pi and M. Sasaki, “Primordial black hole formation in nonminimal curvaton scenarios,” *Phys. Rev. D* **108** no. 10, (2023) L101301, [arXiv:2112.12680 \[astro-ph.CO\]](#).
- [47] W. Barker, B. Gladwyn, and S. Zell, “Inflationary and gravitational wave signatures of small primordial black holes as dark matter,” *Phys. Rev. D* **111** no. 12, (2025) 123033, [arXiv:2410.11948 \[astro-ph.CO\]](#).
- [48] A. Escrivà, F. Kühnel, and Y. Tada, *Primordial black holes*, p. 261–377. Elsevier, 2024. <http://dx.doi.org/10.1016/B978-0-32-395636-9.00012-8>.
- [49] D. G. Figueroa, S. Raatikainen, S. Rasanen, and E. Tomberg, “Non-Gaussian Tail of the Curvature Perturbation in Stochastic Ultraslow-Roll Inflation: Implications for Primordial Black Hole Production,” *Phys. Rev. Lett.* **127** no. 10, (2021) 101302, [arXiv:2012.06551 \[astro-ph.CO\]](#).
- [50] N. Bhaumik and R. K. Jain, “Small scale induced gravitational waves from primordial black holes, a stringent lower mass bound, and the imprints of an early matter to radiation transition,” *Phys. Rev. D* **104** no. 2, (2021) 023531, [arXiv:2009.10424 \[astro-ph.CO\]](#).
- [51] M. Biagetti, V. De Luca, G. Franciolini, A. Kehagias, and A. Riotto, “The formation probability of primordial black holes,” *Phys. Lett. B* **820** (2021) 136602, [arXiv:2105.07810 \[astro-ph.CO\]](#).
- [52] N. Kitajima, Y. Tada, S. Yokoyama, and C.-M. Yoo, “Primordial black holes in peak theory with a non-Gaussian tail,” *JCAP* **10** (2021) 053, [arXiv:2109.00791 \[astro-ph.CO\]](#).
- [53] S. R. Geller, W. Qin, E. McDonough, and D. I. Kaiser, “Primordial black holes from multifield inflation with nonminimal couplings,” *Phys. Rev. D* **106** no. 6, (2022) 063535, [arXiv:2205.04471 \[hep-th\]](#).
- [54] Y.-F. Cai, X.-H. Ma, M. Sasaki, D.-G. Wang, and Z. Zhou, “Highly non-Gaussian tails and primordial black holes from single-field inflation,” *JCAP* **12** (2022) 034, [arXiv:2207.11910 \[astro-ph.CO\]](#).
- [55] S. Choudhury, A. Karde, S. Panda, and M. Sami, “Scalar induced gravity waves from ultra slow-roll galileon inflation,” *Nucl. Phys. B* **1007** (2024) 116678, [arXiv:2308.09273 \[astro-ph.CO\]](#).
- [56] C. Chen, A. Ota, H.-Y. Zhu, and Y. Zhu, “Missing one-loop contributions in secondary gravitational waves,” *Phys. Rev. D* **107** no. 8, (2023) 083518, [arXiv:2210.17176 \[astro-ph.CO\]](#).
- [57] H. Firouzjahi and A. Talebian, “Induced gravitational waves from ultra slow-roll inflation and pulsar timing arrays observations,” *JCAP* **10** (2023) 032, [arXiv:2307.03164 \[gr-qc\]](#).
- [58] L. Frosina and A. Urbano, “Inflationary interpretation of the nHz gravitational-wave background,” *Phys. Rev. D* **108** no. 10, (2023) 103544, [arXiv:2308.06915 \[astro-ph.CO\]](#).
- [59] G. Bhattacharya, S. Choudhury, K. Dey, S. Ghosh, A. Karde, and N. S. Mishra, “Evading no-go for PBH formation and production of SIGWs using Multiple Sharp Transitions in EFT of single field inflation,” *Phys. Dark Univ.* **46** (2024) 101602, [arXiv:2309.00973 \[astro-ph.CO\]](#).
- [60] Y. Tada, T. Terada, and J. Tokuda, “Cancellation of quantum corrections on the soft curvature perturbations,” *JHEP* **01** (2024) 105, [arXiv:2308.04732 \[hep-th\]](#).
- [61] **LISA Cosmology Working Group** Collaboration, E. Bagui *et al.*, “Primordial black holes and their gravitational-wave signatures,” *Living Rev. Rel.* **28** no. 1, (2025) 1, [arXiv:2310.19857 \[astro-ph.CO\]](#).

- [62] W. Qin, S. R. Geller, S. Balaji, E. McDonough, and D. I. Kaiser, “Planck constraints and gravitational wave forecasts for primordial black hole dark matter seeded by multifield inflation,” *Phys. Rev. D* **108** no. 4, (2023) 043508, [arXiv:2303.02168 \[astro-ph.CO\]](#).
- [63] S. Pi, M. Sasaki, V. Takhistov, and J. Wang, “Primordial Black Hole formation from power spectrum with finite-width,” *JCAP* **09** (2025) 045, [arXiv:2501.00295 \[astro-ph.CO\]](#).
- [64] G. Domènech, S. Pi, A. Wang, and J. Wang, “Induced gravitational wave interpretation of PTA data: a complete study for general equation of state,” *JCAP* **08** (2024) 054, [arXiv:2402.18965 \[astro-ph.CO\]](#).
- [65] L. Croney, R. Gregory, and S. Patrick, “Ultra slow-roll with a black hole,” *JCAP* **01** (2025) 096, [arXiv:2411.04806 \[hep-th\]](#).
- [66] H. Firouzjahi and B. Nikbakht, “Hamiltonians to all Orders in Perturbation Theory and Higher Loop Corrections in Single Field Inflation with PBHs Formation,” [arXiv:2502.10287 \[astro-ph.CO\]](#).
- [67] M. Sasaki and J. Wang, “Unveiling Primordial Black Hole Relics Through Induced Gravitational Waves,” [arXiv:2512.22450 \[hep-ph\]](#).
- [68] N. C. Tsamis and R. P. Woodard, “Improved estimates of cosmological perturbations,” *Phys. Rev. D* **69** (2004) 084005, [arXiv:astro-ph/0307463](#).
- [69] W. H. Kinney, “Horizon crossing and inflation with large eta,” *Phys. Rev. D* **72** (2005) 023515, [arXiv:gr-qc/0503017](#).
- [70] J. Martin, H. Motohashi, and T. Suyama, “Ultra Slow-Roll Inflation and the non-Gaussianity Consistency Relation,” *Phys. Rev. D* **87** no. 2, (2013) 023514, [arXiv:1211.0083 \[astro-ph.CO\]](#).
- [71] H. Motohashi, A. A. Starobinsky, and J. Yokoyama, “Inflation with a constant rate of roll,” *JCAP* **09** (2015) 018, [arXiv:1411.5021 \[astro-ph.CO\]](#).
- [72] C. Germani and T. Prokopec, “On primordial black holes from an inflection point,” *Phys. Dark Univ.* **18** (2017) 6–10, [arXiv:1706.04226 \[astro-ph.CO\]](#).
- [73] G. Ballesteros and M. Taoso, “Primordial black hole dark matter from single field inflation,” *Phys. Rev. D* **97** no. 2, (2018) 023501, [arXiv:1709.05565 \[hep-ph\]](#).
- [74] J. Liu, Z.-K. Guo, and R.-G. Cai, “Analytical approximation of the scalar spectrum in the ultraslow-roll inflationary models,” *Phys. Rev. D* **101** no. 8, (2020) 083535, [arXiv:2003.02075 \[astro-ph.CO\]](#).
- [75] S.-L. Cheng, D.-S. Lee, and K.-W. Ng, “Power spectrum of primordial perturbations during ultra-slow-roll inflation with back reaction effects,” *Phys. Lett. B* **827** (2022) 136956, [arXiv:2106.09275 \[astro-ph.CO\]](#).
- [76] D. G. Figueroa, S. Raatikainen, S. Rasanen, and E. Tomberg, “Implications of stochastic effects for primordial black hole production in ultra-slow-roll inflation,” *JCAP* **05** no. 05, (2022) 027, [arXiv:2111.07437 \[astro-ph.CO\]](#).
- [77] S.-L. Cheng, D.-S. Lee, and K.-W. Ng, “Primordial perturbations from ultra-slow-roll single-field inflation with quantum loop effects,” *JCAP* **03** (2024) 008, [arXiv:2305.16810 \[astro-ph.CO\]](#).
- [78] M. P. Hertzberg and M. Yamada, “Primordial Black Holes from Polynomial Potentials in Single Field Inflation,” *Phys. Rev. D* **97** no. 8, (2018) 083509, [arXiv:1712.09750 \[astro-ph.CO\]](#).
- [79] C. Pattison, V. Vennin, H. Assadullahi, and D. Wands, “The attractive behaviour of ultra-slow-roll inflation,” *JCAP* **08** (2018) 048, [arXiv:1806.09553 \[astro-ph.CO\]](#).
- [80] G. Ballesteros, J. Rey, M. Taoso, and A. Urbano, “Stochastic inflationary dynamics beyond slow-roll and consequences for primordial black hole formation,” *JCAP* **08** (2020) 043, [arXiv:2006.14597 \[astro-ph.CO\]](#).
- [81] V. Vennin, *Stochastic inflation and primordial black holes*. PhD thesis, U. Paris-Saclay, 6, 2020. [arXiv:2009.08715 \[astro-ph.CO\]](#).
- [82] C. Pattison, V. Vennin, D. Wands, and H. Assadullahi, “Ultra-slow-roll inflation with quantum diffusion,” *JCAP* **04** (2021) 080, [arXiv:2101.05741 \[astro-ph.CO\]](#).
- [83] A. Karam, N. Koivunen, E. Tomberg, V. Vaskonen, and H. Veermäe, “Anatomy of single-field inflationary models for primordial black holes,” *JCAP* **03** (2023) 013, [arXiv:2205.13540 \[astro-ph.CO\]](#).
- [84] S. Pi and M. Sasaki, “Logarithmic Duality of the Curvature Perturbation,” *Phys. Rev. Lett.* **131** no. 1, (2023) 011002, [arXiv:2211.13932 \[astro-ph.CO\]](#).
- [85] H. Firouzjahi, “Revisiting loop corrections in single field ultraslow-roll inflation,” *Phys. Rev. D* **109** no. 4, (2024) 043514, [arXiv:2311.04080 \[astro-ph.CO\]](#).
- [86] R. Kawaguchi, S. Tsujikawa, and Y. Yamada, “Proving the absence of large one-loop corrections to the power spectrum of curvature perturbations in transient ultra-slow-roll inflation within the path-integral approach,” *JHEP* **12** (2024) 095, [arXiv:2407.19742 \[hep-th\]](#).
- [87] T. Fujita, R. Kawaguchi, M. Sasaki, and Y. Tada, “Dip and non-linearity in the curvature perturbation from inflation with a transient non-slow-roll stage,” *JCAP* **09** (2025) 046, [arXiv:2503.19744 \[astro-ph.CO\]](#).
- [88] G. Franciolini, A. Iovino, Junior., M. Taoso, and A. Urbano, “Perturbativity in the presence of ultraslow-roll dynamics,” *Phys. Rev. D* **109** no. 12, (2024) 123550, [arXiv:2305.03491 \[astro-ph.CO\]](#).
- [89] S. Choudhury, S. Panda, and M. Sami, “Galileon inflation evades the no-go for PBH formation in the single-field framework,” *JCAP* **08** (2023) 078, [arXiv:2304.04065 \[astro-ph.CO\]](#).
- [90] S. S. Mishra, E. J. Copeland, and A. M. Green, “Primordial black holes and stochastic inflation beyond slow roll. Part I. Noise matrix elements,” *JCAP* **09** (2023) 005, [arXiv:2303.17375 \[astro-ph.CO\]](#).
- [91] G. Ballesteros and J. Gambín Egea, “One-loop power spectrum in ultra slow-roll inflation and implications for primordial black hole dark matter,” *JCAP* **07** (2024) 052, [arXiv:2404.07196 \[astro-ph.CO\]](#).
- [92] D. Artigas, S. Pi, and T. Tanaka, “Extended δN Formalism: Nonspatially Flat Separate-Universe Approach,” *Phys. Rev. Lett.* **134** no. 22, (2025) 221001, [arXiv:2408.09964 \[astro-ph.CO\]](#).
- [93] R. Inui, H. Motohashi, S. Pi, Y. Tada, and S. Yokoyama, “Constant roll and non-Gaussian tail in light of logarithmic duality,” *JCAP* **02** (2025) 042, [arXiv:2409.13500 \[astro-ph.CO\]](#).
- [94] A. Escrivà, J. Garriga, and S. Pi, “Inflationary relics from an ultra-slow-roll plateau,” *JCAP* **03** (2026) 018, [arXiv:2512.04986 \[astro-ph.CO\]](#).

- [95] Z. Yi and Y. Gong, “On the constant-roll inflation,” *JCAP* **03** (2018) 052, [arXiv:1712.07478 \[gr-qc\]](#).
- [96] M. J. P. Morse and W. H. Kinney, “Large- η constant-roll inflation is never an attractor,” *Phys. Rev. D* **97** no. 12, (2018) 123519, [arXiv:1804.01927 \[astro-ph.CO\]](#).
- [97] P. Carrilho, K. A. Malik, and D. J. Mulryne, “Dissecting the growth of the power spectrum for primordial black holes,” *Phys. Rev. D* **100** no. 10, (2019) 103529, [arXiv:1907.05237 \[astro-ph.CO\]](#).
- [98] H. Motohashi, S. Mukohyama, and M. Oliosi, “Constant Roll and Primordial Black Holes,” *JCAP* **03** (2020) 002, [arXiv:1910.13235 \[gr-qc\]](#).
- [99] S. Choudhury, S. Panda, and M. Sami, “PBH formation in EFT of single field inflation with sharp transition,” *Phys. Lett. B* **845** (2023) 138123, [arXiv:2302.05655 \[astro-ph.CO\]](#).
- [100] H. Motohashi and Y. Tada, “Squeezed bispectrum and one-loop corrections in transient constant-roll inflation,” *JCAP* **08** (2023) 069, [arXiv:2303.16035 \[astro-ph.CO\]](#).
- [101] N. Bhaumik and R. K. Jain, “Primordial black holes dark matter from inflection point models of inflation and the effects of reheating,” *JCAP* **01** (2020) 037, [arXiv:1907.04125 \[astro-ph.CO\]](#).
- [102] E. Tomberg and K. Dimopoulos, “Eternal inflation near inflection points: a challenge to primordial black hole models,” *JCAP* **01** (2026) 033, [arXiv:2507.15522 \[astro-ph.CO\]](#).
- [103] H. Motohashi and W. Hu, “Primordial Black Holes and Slow-Roll Violation,” *Phys. Rev. D* **96** no. 6, (2017) 063503, [arXiv:1706.06784 \[astro-ph.CO\]](#).
- [104] K. Kannike, L. Marzola, M. Raidal, and H. Veermäe, “Single Field Double Inflation and Primordial Black Holes,” *JCAP* **09** (2017) 020, [arXiv:1705.06225 \[astro-ph.CO\]](#).
- [105] S. S. Bhatt, S. S. Mishra, S. Basak, and S. N. Sahoo, “Numerical simulations of inflationary dynamics: Slow roll and beyond,” *SciPost Phys. Codeb.* **42** (2024) 1, [arXiv:2212.00529 \[gr-qc\]](#).
- [106] A. Caravano, G. Franciolini, and S. Renaux-Petel, “Ultraslow-roll inflation on the lattice: Backreaction and nonlinear effects,” *Phys. Rev. D* **111** no. 6, (2025) 063518, [arXiv:2410.23942 \[astro-ph.CO\]](#).
- [107] A. Caravano, G. Franciolini, and S. Renaux-Petel, “Ultraslow-roll inflation on the lattice. II. Nonperturbative curvature perturbation,” *Phys. Rev. D* **112** no. 8, (2025) 083508, [arXiv:2506.11795 \[astro-ph.CO\]](#).
- [108] S. Allegrini, A. J. Iovino, and H. Veermäe, “Beware of the running n_s when producing heavy primordial black holes,” [arXiv:2510.18791 \[astro-ph.CO\]](#).
- [109] C. T. Byrnes, P. S. Cole, and S. P. Patil, “Steepest growth of the power spectrum and primordial black holes,” *JCAP* **06** (2019) 028, [arXiv:1811.11158 \[astro-ph.CO\]](#).
- [110] K. Inomata, M. Kawasaki, K. Mukaida, and T. T. Yanagida, “Double inflation as a single origin of primordial black holes for all dark matter and LIGO observations,” *Phys. Rev. D* **97** no. 4, (2018) 043514, [arXiv:1711.06129 \[astro-ph.CO\]](#).
- [111] S. Passaglia, W. Hu, and H. Motohashi, “Primordial black holes and local non-Gaussianity in canonical inflation,” *Phys. Rev. D* **99** no. 4, (2019) 043536, [arXiv:1812.08243 \[astro-ph.CO\]](#).
- [112] G. Tasinato, “An analytic approach to non-slow-roll inflation,” *Phys. Rev. D* **103** no. 2, (2021) 023535, [arXiv:2012.02518 \[hep-th\]](#).
- [113] J. M. Ezquiaga and J. García-Bellido, “Quantum diffusion beyond slow-roll: implications for primordial black-hole production,” *JCAP* **08** (2018) 018, [arXiv:1805.06731 \[astro-ph.CO\]](#).
- [114] G. Franciolini and A. Urbano, “Primordial black hole dark matter from inflation: The reverse engineering approach,” *Phys. Rev. D* **106** no. 12, (2022) 123519, [arXiv:2207.10056 \[astro-ph.CO\]](#).
- [115] P. Adshead, W. Hu, and V. Miranda, “Bispectrum in Single-Field Inflation Beyond Slow-Roll,” *Phys. Rev. D* **88** no. 2, (2013) 023507, [arXiv:1303.7004 \[astro-ph.CO\]](#).
- [116] H. V. Ragavendra and L. Sriramkumar, “Observational Imprints of Enhanced Scalar Power on Small Scales in Ultra Slow Roll Inflation and Associated Non-Gaussianities,” *Galaxies* **11** no. 1, (2023) 34, [arXiv:2301.08887 \[astro-ph.CO\]](#).
- [117] D. Cruces, C. Germani, and T. Prokopec, “Failure of the stochastic approach to inflation beyond slow-roll,” *JCAP* **03** (2019) 048, [arXiv:1807.09057 \[gr-qc\]](#).
- [118] C. Pattison, V. Vennin, H. Assadullahi, and D. Wands, “Stochastic inflation beyond slow roll,” *JCAP* **07** (2019) 031, [arXiv:1905.06300 \[astro-ph.CO\]](#).
- [119] D. Sharma, “Stochastic inflation and non-perturbative power spectrum beyond slow roll,” *JCAP* **03** (2025) 017, [arXiv:2411.08854 \[astro-ph.CO\]](#).
- [120] B.-Y. Su, N. Li, and L. Feng, “Primordial black holes from the ultraslow-roll phase in the inflaton-curvaton mixed field inflation,” *Eur. Phys. J. C* **85** no. 2, (2025) 197, [arXiv:2502.14323 \[astro-ph.CO\]](#).
- [121] S. Pi and J. Wang, “Primordial black hole formation in Starobinsky’s linear potential model,” *JCAP* **06** (2023) 018, [arXiv:2209.14183 \[astro-ph.CO\]](#).
- [122] S. Maity, H. V. Ragavendra, S. K. Sethi, and L. Sriramkumar, “Loop contributions to the scalar power spectrum due to quartic order action in ultra slow roll inflation,” *JCAP* **05** (2024) 046, [arXiv:2307.13636 \[astro-ph.CO\]](#).
- [123] Y.-F. Cai, X. Chen, M. H. Namjoo, M. Sasaki, D.-G. Wang, and Z. Wang, “Revisiting non-Gaussianity from non-attractor inflation models,” *JCAP* **05** (2018) 012, [arXiv:1712.09998 \[astro-ph.CO\]](#).
- [124] I. Dalianis, A. Kehagias, and G. Tringas, “Primordial black holes from α -attractors,” *JCAP* **01** (2019) 037, [arXiv:1805.09483 \[astro-ph.CO\]](#).
- [125] G. Ballesteros, J. Rey, M. Taoso, and A. Urbano, “Primordial black holes as dark matter and gravitational waves from single-field polynomial inflation,” *JCAP* **07** (2020) 025, [arXiv:2001.08220 \[astro-ph.CO\]](#).
- [126] L. Iacconi, H. Assadullahi, M. Fasiello, and D. Wands, “Revisiting small-scale fluctuations in α -attractor models of inflation,” *JCAP* **06** no. 06, (2022) 007, [arXiv:2112.05092 \[astro-ph.CO\]](#).
- [127] P. S. Cole, A. D. Gow, C. T. Byrnes, and S. P. Patil, “Smooth vs instant inflationary transitions: steepest growth re-examined and primordial black holes,” *JCAP* **05** (2024) 022, [arXiv:2204.07573 \[astro-ph.CO\]](#).

- [128] J. H. P. Jackson, H. Assadullahi, A. D. Gow, K. Koyama, V. Vennin, and D. Wands, “The separate-universe approach and sudden transitions during inflation,” *JCAP* **05** (2024) 053, [arXiv:2311.03281 \[astro-ph.CO\]](#).
- [129] M. W. Davies, L. Iacconi, and D. J. Mulryne, “Numerical 1-loop correction from a potential yielding ultra-slow-roll dynamics,” *JCAP* **04** (2024) 050, [arXiv:2312.05694 \[astro-ph.CO\]](#).
- [130] J. H. P. Jackson, H. Assadullahi, A. D. Gow, K. Koyama, V. Vennin, and D. Wands, “Stochastic inflation beyond slow roll: noise modelling and importance sampling,” *JCAP* **04** (2025) 073, [arXiv:2410.13683 \[astro-ph.CO\]](#).
- [131] V. Briaud, A. Karam, N. Koivunen, E. Tomberg, H. Veermäe, and V. Vennin, “How deep is the dip and how tall are the wiggles in inflationary power spectra?,” *JCAP* **05** (2025) 097, [arXiv:2501.14681 \[astro-ph.CO\]](#).
- [132] V. F. Mukhanov, “Gravitational Instability of the Universe Filled with a Scalar Field,” *JETP Lett.* **41** (1985) 493–496.
- [133] M. Sasaki, “Large Scale Quantum Fluctuations in the Inflationary Universe,” *Prog. Theor. Phys.* **76** (1986) 1036.
- [134] E. D. Stewart and D. H. Lyth, “A More accurate analytic calculation of the spectrum of cosmological perturbations produced during inflation,” *Phys. Lett. B* **302** (1993) 171–175, [arXiv:gr-qc/9302019](#).
- [135] X. Chen, M.-x. Huang, S. Kachru, and G. Shiu, “Observational signatures and non-Gaussianities of general single field inflation,” *JCAP* **01** (2007) 002, [arXiv:hep-th/0605045](#).
- [136] J. Kristiano and J. Yokoyama, *Generating Large Primordial Fluctuations in Single-Field Inflation for Primordial Black Hole Formation*, p. 53–91. Springer Nature Singapore, 2025. http://dx.doi.org/10.1007/978-981-97-8887-3_3.
- [137] L. Anguelova, P. Suranyi, and L. C. R. Wijewardhana, “Systematics of Constant Roll Inflation,” *JCAP* **02** (2018) 004, [arXiv:1710.06989 \[hep-th\]](#).
- [138] H. Motohashi and A. A. Starobinsky, “Constant-roll inflation: confrontation with recent observational data,” *EPL* **117** no. 3, (2017) 39001, [arXiv:1702.05847 \[astro-ph.CO\]](#).
- [139] S. D. Odintsov and V. K. Oikonomou, “Inflation with a Smooth Constant-Roll to Constant-Roll Era Transition,” *Phys. Rev. D* **96** no. 2, (2017) 024029, [arXiv:1704.02931 \[gr-qc\]](#).
- [140] M. Guerrero, D. Rubiera-Garcia, and D. Saez-Chillon Gomez, “Constant roll inflation in multifield models,” *Phys. Rev. D* **102** (2020) 123528, [arXiv:2008.07260 \[gr-qc\]](#).
- [141] S. M. Ahmadi, N. Ahmadi, and M. Shokri, “Analytical insights into constant-roll condition: extending the paradigm to non-canonical models,” *JCAP* **05** (2024) 005, [arXiv:2312.05998 \[gr-qc\]](#).
- [142] J. Kristiano and J. Yokoyama, “Comparing sharp and smooth transitions of the second slow-roll parameter in single-field inflation,” *JCAP* **10** (2024) 036, [arXiv:2405.12145 \[astro-ph.CO\]](#).
- [143] H. Motohashi, “Constant-Roll Inflation,” 4, 2025. [arXiv:2504.16757 \[astro-ph.CO\]](#).
- [144] O. Özsoy and G. Tasinato, “On the slope of the curvature power spectrum in non-attractor inflation,” *JCAP* **04** (2020) 048, [arXiv:1912.01061 \[astro-ph.CO\]](#).
- [145] G. Domènech, G. Vargas, and T. Vargas, “An exact model for enhancing/suppressing primordial fluctuations,” *JCAP* **03** (2024) 002, [arXiv:2309.05750 \[astro-ph.CO\]](#).
- [146] E. Tomberg, “Numerical stochastic inflation constrained by frozen noise,” *JCAP* **04** (2023) 042, [arXiv:2210.17441 \[astro-ph.CO\]](#).
- [147] L. Iacconi, D. Mulryne, and D. Seery, “Loop corrections in the separate universe picture,” *JCAP* **06** (2024) 062, [arXiv:2312.12424 \[astro-ph.CO\]](#).
- [148] K. Kohri and T. Terada, “Semianalytic calculation of gravitational wave spectrum nonlinearly induced from primordial curvature perturbations,” *Phys. Rev. D* **97** no. 12, (2018) 123532, [arXiv:1804.08577 \[gr-qc\]](#).
- [149] J. R. Espinosa, D. Racco, and A. Riotto, “A Cosmological Signature of the SM Higgs Instability: Gravitational Waves,” *JCAP* **09** (2018) 012, [arXiv:1804.07732 \[hep-ph\]](#).
- [150] V. Dandoy, V. Domcke, and F. Rompineve, “Search for scalar induced gravitational waves in the international pulsar timing array data release 2 and NANOgrav 12.5 years datasets,” *SciPost Phys. Core* **6** (2023) 060, [arXiv:2302.07901 \[astro-ph.CO\]](#).
- [151] C.-Z. Li, C. Yuan, and Q.-g. Huang, “Gravitational waves induced by scalar perturbations with a broken power-law peak,” *JCAP* **01** (2025) 067, [arXiv:2407.12914 \[gr-qc\]](#).
- [152] **MACHO** Collaboration, P. Popowski *et al.*, “Microlensing optical depth towards the galactic bulge using clump giants from the MACHO survey,” *Astrophys. J.* **631** (2005) 879–905, [arXiv:astro-ph/0410319](#).
- [153] **OGLE** Collaboration, S. Kozłowski *et al.*, “Quantifying Quasar Variability As Part of a General Approach To Classifying Continuously Varying Sources,” *Astrophys. J.* **708** (2010) 927–945, [arXiv:0909.1326 \[astro-ph.CO\]](#).
- [154] **MOA** Collaboration, T. Sumi *et al.*, “The Microlensing Event Rate and Optical Depth Toward the Galactic Bulge from MOA-II,” *Astrophys. J.* **778** (2013) 150, [arXiv:1305.0186 \[astro-ph.GA\]](#).
- [155] **DES** Collaboration, A. J. Shajib *et al.*, “Is every strong lens model unhappy in its own way? Uniform modelling of a sample of 13 quadruply+ imaged quasars,” *Mon. Not. Roy. Astron. Soc.* **483** no. 4, (2019) 5649–5671, [arXiv:1807.09278 \[astro-ph.GA\]](#). [Erratum: *Mon. Not. Roy. Astron. Soc.* 501, 2833–2835 (2021)].
- [156] **LSST Dark Energy Science** Collaboration, V. G. Shah, A. Gagliano, K. Malanchev, G. Narayan, and A. I. Malz, “ORACLE: A Real-time, Hierarchical, Deep Learning Photometric Classifier for the LSST,” *Astrophys. J.* **995** no. 1, (2025) 4, [arXiv:2501.01496 \[astro-ph.IM\]](#).
- [157] **WMAP** Collaboration, E. Komatsu *et al.*, “Seven-Year Wilkinson Microwave Anisotropy Probe (WMAP) Observations: Cosmological Interpretation,” *Astrophys. J. Suppl.* **192** (2011) 18, [arXiv:1001.4538 \[astro-ph.CO\]](#).

- [158] **BICEP2, Keck Array** Collaboration, P. A. R. Ade *et al.*, “Improved Constraints on Cosmology and Foregrounds from BICEP2 and Keck Array Cosmic Microwave Background Data with Inclusion of 95 GHz Band,” *Phys. Rev. Lett.* **116** (2016) 031302, [arXiv:1510.09217 \[astro-ph.CO\]](#).
- [159] **Planck** Collaboration, N. Aghanim *et al.*, “Planck 2018 results. VI. Cosmological parameters,” *Astron. Astrophys.* **641** (2020) A6, [arXiv:1807.06209 \[astro-ph.CO\]](#). [Erratum: *Astron. Astrophys.* 652, C4 (2021)].
- [160] **LiteBIRD** Collaboration, P. Campeti *et al.*, “LiteBIRD science goals and forecasts. A case study of the origin of primordial gravitational waves using large-scale CMB polarization,” *JCAP* **06** (2024) 008, [arXiv:2312.00717 \[astro-ph.CO\]](#).
- [161] **SPT-3G** Collaboration, A. R. Khalife *et al.*, “SPT-3G D1: Axion Early Dark Energy with CMB experiments and DESI,” [arXiv:2507.23355 \[astro-ph.CO\]](#).
- [162] **Atacama Cosmology Telescope** Collaboration, T. Louis *et al.*, “The Atacama Cosmology Telescope: DR6 power spectra, likelihoods and Λ CDM parameters,” *JCAP* **11** (2025) 062, [arXiv:2503.14452 \[astro-ph.CO\]](#).
- [163] **LIGO Scientific** Collaboration, P. J. Sutton, “Searching for gravitational waves with LIGO,” *J. Phys. Conf. Ser.* **110** (2008) 062024.
- [164] **KAGRA** Collaboration, K. Kokeyama, “Observing the Universe from Underground Gravitational Wave Telescope KAGRA,” in *3rd World Summit on Exploring the Dark Side of the Universe*, pp. 41–48. 2020.
- [165] **NANOGrav** Collaboration, Z. Arzoumanian *et al.*, “The NANOGrav 12.5 yr Data Set: Bayesian Limits on Gravitational Waves from Individual Supermassive Black Hole Binaries,” *Astrophys. J. Lett.* **951** no. 2, (2023) L28, [arXiv:2301.03608 \[astro-ph.GA\]](#).
- [166] **DECIGO** Collaboration, S. Kawamura, “Space gravitational wave antenna DECIGO and B-DECIGO,” in *16th Marcel Grossmann Meeting on Recent Developments in Theoretical and Experimental General Relativity, Astrophysics and Relativistic Field Theories*. 2023.
- [167] **LIGO Scientific, KAGRA, Virgo, Swift, Swift-BAT/GUANO** Collaboration, G. Raman *et al.*, “Swift-BAT GUANO Follow-up of Gravitational-wave Triggers in the Third LIGO–Virgo–KAGRA Observing Run,” *Astrophys. J.* **980** no. 2, (2025) 207, [arXiv:2407.12867 \[astro-ph.HE\]](#).
- [168] **ET** Collaboration, A. Abac *et al.*, “The Science of the Einstein Telescope,” [arXiv:2503.12263 \[gr-qc\]](#).
- [169] **Taiji Scientific** Collaboration, Y.-L. Wu *et al.*, “China’s first step towards probing the expanding universe and the nature of gravity using a space borne gravitational wave antenna,” *Commun. Phys.* **4** no. 1, (2021) 34.
- [170] **TianQin** Collaboration, J. Mei *et al.*, “The TianQin project: current progress on science and technology,” *PTEP* **2021** no. 5, (2021) 05A107, [arXiv:2008.10332 \[gr-qc\]](#).
- [171] “*NIST Digital Library of Mathematical Functions.*” <https://dlmf.nist.gov/>.

Appendix A: Coefficients of solutions

In this appendix, we provide the explicit expressions for all coefficients in the analytical solutions presented in the main text.

- *coefficients of $\epsilon_2(N)$:*

ϵ_2 satisfies Eq. (5), a first-order ordinary differential equation, together with the boundary condition $\epsilon_2(\tau_\star) = 0$, the solution can be fixed as

$$\epsilon_2(N) = e^{-N} \frac{\mathcal{G}_1(0) \cdot \mathcal{G}_2(N) - \mathcal{G}_2(0) \cdot \mathcal{G}_1(N)}{\mathcal{G}_1(0) \cdot \mathcal{G}_4(N) + \mathcal{G}_2(0) \cdot \mathcal{G}_3(N)}, \quad (\text{A1})$$

where functions $\mathcal{G}_i(N)$ are

$$\mathcal{G}_1(N) = [e^N(3 + 2\mu) - 2q] U \left[\frac{1}{2} - \frac{\alpha}{2q} + \mu, 1 + 2\mu, 2q e^{-N} \right] + 2(\alpha - q - 2q\mu) U \left[\frac{3}{2} - \frac{\alpha}{2q} + \mu, 2 + 2\mu, 2q e^{-N} \right], \quad (\text{A2})$$

$$\mathcal{G}_2(N) = 4q L_{\alpha/2q-\mu-3/2}^{1+2\mu}(2q e^{-N}) - [e^N(2\mu + 3) - 2q] L_{\alpha/2q-\mu-1/2}^{2\mu}(2q e^{-N}), \quad (\text{A3})$$

$$\mathcal{G}_3(N) = U \left[\frac{1}{2} - \frac{\alpha}{2q} + \mu, 1 + 2\mu, 2q e^{-N} \right], \quad (\text{A4})$$

$$\mathcal{G}_4(N) = L_{\alpha/2q-1/2-\mu}^{2\mu}(2q e^{-N}), \quad (\text{A5})$$

here $U(a, b, z)$ is the confluent Hypergeometric- U function, while $L_n^a(z)$ is the generalised Laguerre polynomial.

- *coefficients of $z(\tau)$:*

The solution is given by Eq. (8), and the coefficients are

$$\mathcal{B}_1 = \frac{\sqrt{2\epsilon_{\text{SR1}}} M_{\text{pl}}}{H_0 \tau_\star} \frac{(\alpha - 2q - 2q^2)M_0 - (\alpha + q + 2\mu q)M_1}{(\alpha + q + 2\mu q)M_1 W_0 + 2q M_0 W_1}, \quad (\text{A6})$$

$$\mathcal{B}_2 = -\frac{\sqrt{2\epsilon_{\text{SR1}}} M_{\text{pl}}}{H_0 \tau_\star} \frac{(\alpha - 2q - 2q^2)W_0 + 2q W_1}{(\alpha + q + 2\mu q)M_1 W_0 + 2q M_0 W_1}, \quad (\text{A7})$$

where we have introduced the shorthand notations as

$$W_n \equiv W_{\frac{\alpha}{2q}+n,\mu}(2q), \quad M_n \equiv M_{\frac{\alpha}{2q}+n,\mu}(2q). \quad (\text{A8})$$

- *coefficients of $v_k(\tau)$:*

The solution of MS variable $v_k(\tau)$ is given by Eq. (6), and the coefficients are

$$\mathcal{C}_1(k) = \frac{e^{-ik\tau_\star}}{\sqrt{2}k^{3/2}\tau_\star \mathcal{Y}_0} \left\{ \left[-i\frac{\alpha}{\tau_\star} + (1 + 2\mu)k_{\text{eff}} \right] (-i + k\tau_\star) \widetilde{M}_1 + \left[(1 + ik\tau_\star) \left(2k_{\text{eff}}(k + k_{\text{eff}})\tau_\star + \frac{\alpha}{\tau_\star} \right) - 2ik_{\text{eff}} \right] \widetilde{M}_0 \right\}, \quad (\text{A9})$$

$$\mathcal{C}_2(k) = \frac{e^{-ik\tau_\star}}{\sqrt{2}k^{3/2}\tau_\star \mathcal{Y}_0} \left\{ \left[2ik_{\text{eff}} + (1 + ik\tau_\star) \left(-\frac{\alpha}{\tau_\star} - 2k_{\text{eff}}(k + k_{\text{eff}})\tau_\star \right) \right] \widetilde{W}_0 - 2ik_{\text{eff}}(1 + ik\tau_\star) \widetilde{W}_1 \right\}, \quad (\text{A10})$$

we also defined the shorthand notations as

$$\widetilde{W}_n \equiv W_{i\tilde{\alpha}+n,\mu}(2ik_{\text{eff}}\tau_\star), \quad \widetilde{M}_n \equiv M_{i\tilde{\alpha}+n,\mu}(2ik_{\text{eff}}\tau_\star), \quad (\text{A11})$$

and the factor \mathcal{Y}_0 in the denominator then can be expressed as

$$\mathcal{Y}_0 = 2k_{\text{eff}} \widetilde{W}_1 \widetilde{M}_0 + \left[-i\frac{\alpha}{\tau_\star} + (1 + 2\mu)k_{\text{eff}} \right] \widetilde{W}_0 \widetilde{M}_1. \quad (\text{A12})$$

Appendix B: Approximation formulae in different regions

First of all, to obtain the final power spectrum Eq. (12), we have used the asymptotic behaviour of Whittaker functions:

$$\lim_{z \rightarrow 0} M_{\kappa, \mu}(z) = z^{\frac{1}{2} + \mu}, \quad (\text{B1})$$

$$\lim_{z \rightarrow 0} W_{\kappa, \mu}(z) = z^{\frac{1}{2} - \mu} \frac{\Gamma(2\mu)}{\Gamma(1/2 - \kappa + \mu)} + z^{\frac{1}{2} + \mu} \frac{\Gamma(-2\mu)}{\Gamma(1/2 - \kappa - \mu)}, \quad (\text{B2})$$

in the case $\mu > 0$, the dominant contribution arises from the $z^{1/2 - \mu}$ term of the Whittaker- W , Eq. (12) then reduces to a ratio of Euler Gamma functions.

- *IR region:*

In the IR region $k/k_* \ll 1$, we first take $k_{\text{eff}} \rightarrow iqk_*$ in the Whittaker functions¹ and then perform the expansion around $k = 0$, which yields a quadratic function, whose coefficients are given as

$$a_0 = \frac{1}{2\tau_*^2} \left[\frac{M_0(\alpha - 2q - 2q^2) - M_1(\alpha + q + 2\mu q)}{2q M_0 W_1 + M_1 W_0(\alpha + q + 2\mu q)} \right]^2, \quad (\text{B3})$$

$$\frac{a_2}{a_0} = \tau_*^2 \frac{(\alpha + q + 2\mu q) M_1 + (2q^2 - 2q - \alpha) M_0}{(\alpha + q + 2\mu q) M_1 + (2q^2 + 2q - \alpha) M_0}. \quad (\text{B4})$$

- *Growth region:*

For the k^4 -growth region, the key quantity is the dip position which can be determined from the expressions for a_i above. To analyse the other growth behavior, we need the power spectrum evaluated at $k = q$. At first glance, this may appear problematic, since $k_{\text{eff}} \rightarrow 0$ and then the Whittaker-function parameter $\tilde{\alpha}$ is divergent. To evaluate it properly, we need to use the following asymptotic formula [171],

$$\lim_{\kappa \rightarrow \infty} M_{\kappa, \mu}(x) = \kappa^{-\mu} \sqrt{x} \Gamma(2\mu + 1) J_{2\mu}(2\sqrt{x\kappa}), \quad (\text{B5})$$

$$\lim_{\kappa \rightarrow \infty} W_{\kappa, \mu}(x) = \sqrt{x} \Gamma(\kappa + 1/2) \left[\sin \pi(\kappa - \mu) J_{2\mu}(2\sqrt{x\kappa}) - \cos \pi(\kappa - \mu) Y_{2\mu}(2\sqrt{x\kappa}) \right], \quad (\text{B6})$$

here $J_\mu(x)$ and $Y_\mu(x)$ are the Bessel functions of the first and second kinds, respectively. Then we can get the power spectrum

$$\begin{aligned} & \mathcal{P}_{\mathcal{R}}(qk_*) \\ &= \frac{(2q)^{2\mu-1}}{|4\pi\tau_*\mathcal{B}_1|^2} \Gamma\left(\frac{1}{2} - \frac{\alpha}{2q} + \mu\right)^2 \left| \left((3 + 2\mu)(i - q) - 2iq^2 \right) {}_0\mathbf{F}_1(; 2\mu + 1; -\alpha) - 2\alpha(i - q) {}_0\mathbf{F}_1(; 2\mu + 2; -\alpha) \right|^2, \end{aligned} \quad (\text{B7})$$

where ${}_0\mathbf{F}_1(; a; z)$ is a regularised confluent Hypergeometric function.

- *UV region:*

In the region $k/k_* \gg 1$, the parameter appearing in the special functions becomes $\tilde{\alpha} \rightarrow 0$. This makes it straightforward to expand the power spectrum in the UV region, yielding

$$\mathcal{C}_1(k) \sim \frac{1}{\sqrt{2k}}, \quad (\text{B8})$$

and $k_{\text{eff}} \rightarrow k$ in the Gamma functions, then we can readily obtain the final approximation Eq. (17).

¹ Strictly speaking, we have to perform the expansion while keeping the k -dependence in both the parameters and the arguments of the Whittaker functions, which would lead to more complicated expressions involving derivatives of the Whittaker functions with respect to their parameters. But we have checked that the approximated results have at most percent-level errors

for the parameters chosen in our study, which does not affect our main results and conclusion, so we adopt this approximation for simpler expression. Moreover, some software do not provide built-in functions for direct evaluation of the derivatives of the Whittaker functions.

Appendix C: The approximation of the scale factor

In this appendix, we justify the approximation $a = -1/H_0\tau$, $N = -\ln(\tau/\tau_*)$ in our analysis. By definition, the e -fold number is

$$N \equiv \ln \frac{a}{a_0}, \quad (\text{C1})$$

which allows us to write down

$$a = a_0 e^N, \quad dN = H dt. \quad (\text{C2})$$

Therefore, the first slow-roll parameter is given by

$$\epsilon_1 \equiv -\frac{\dot{H}}{H^2} = -\frac{d \ln H}{dN}, \quad (\text{C3})$$

which can be solved as

$$H = H_0 \exp\left(-\int \epsilon_1 dN\right). \quad (\text{C4})$$

As a result, the conformal time can be expressed as

$$\tau = \int \frac{dt}{a} = \int \frac{dN}{aH} = \int \frac{dN}{aH_0} \exp\left(\int^N \epsilon_1 dN'\right) = \int \frac{dN}{a_0 H_0} e^{-N} \sum_{n=0}^{\infty} \frac{1}{n!} \left(\int^N \epsilon_1 dN'\right)^n. \quad (\text{C5})$$

For the exact de Sitter case, $\epsilon_1 = 0$ such that

$$\tau = -\frac{1}{aH_0}. \quad (\text{C6})$$

Slow-roll correction comes from the higher order terms in the Taylor expansion. These terms can be safely dropped as long as parameters are properly chosen such that

$$\left|\int \epsilon_1 dN\right| \ll 1, \quad (\text{C7})$$

which is exactly the case in the main text.

Appendix D: Other choices of parameters

μ	α	N_1	N_{eff}	Max $\mathcal{P}_{\mathcal{R}}$
2.2407	25.860	0.720	1.90	1.92×10^{-3}
2.1681	24.730	0.735	2.00	3.59×10^{-3}
2.0976	23.650	0.750	2.06	5.45×10^{-3}
2.0294	22.630	0.766	2.19	1.18×10^{-2}
1.9633	21.660	0.781	2.34	3.07×10^{-2}
1.8991	20.735	0.797	2.47	7.18×10^{-2}
1.8368	19.855	0.814	2.63	1.84×10^{-1}
1.7764	19.018	0.830	2.82	6.24×10^{-1}

TABLE I. Peak amplitudes for different parameter choices. In order to make connection with USR, the parameters are fine-tuned such that the minimum value of ϵ_2 is -6 . Here μ and α are parameters in our smooth transition model, while N_1 and N_{eff} are parameters in the sharp transition counterpart.

Tab. I summarizes several representative examples in which ϵ_2 reaches the critical value -6 , together with the corresponding peak amplitude $\max \mathcal{P}_{\mathcal{R}}$. Demanding that PBHs are not overproduced sets an upper limit on the peak amplitudes, which in turn imposes a lower bound on the parameter μ in our model. As shown in the table, values $\mu \gtrsim 2$ are preferred.